Chinese Chemical Letters 35 (2024) 108808

Contents lists available at ScienceDirect

Chinese Chemical Letters

journal homepage: www.elsevier.com/locate/cclet

Copper coordination-driven self-assembly and encapsulation of PCR reagents

Chang Lu[a,b], Jinkai Zheng[a,*], Juewen Liu[b,*]

[a] Institute of Food Science and Technology, Chinese Academy of Agricultural Sciences, Beijing 100193, China
[b] Department of Chemistry, Waterloo Institute for Nanotechnology, University of Waterloo, Waterloo, ON, N2L 3G1, Canada

ARTICLE INFO

Article history:
Received 18 October 2022
Revised 11 July 2023
Accepted 13 July 2023
Available online 14 July 2023

Keywords:
Metal ions
Coordination
Encapsulation
PCR
Storage

ABSTRACT

Polymerase chain reactions (PCR) are a very important tool for use in cloning, nucleic acid sequencing and diagnostic testing. The storage conditions of PCR reagents are limited to freezing and a lot of mixing steps are needed. In this paper, we report using metal ions to form coordination nanomaterials with the intrinsic components of the PCR reagents including dNTP, DNA primers and DNA polymerase as an integrated PCR reaction system. To complete PCR reactions, users need only to dissolve the coordination nanomaterials with a buffer and add template DNA. A few transition metal ions were screened and Cu^{2+} was found to be the most effective metal ion for this purpose. Then the encapsulation efficiency of PCR reagents was measured, which can reach close to 100% for the primers and DNA polymerase, but only 10% for dNTP because dNTP was excess. Further study also exhibited this integrated PCR reaction system can be used for DNA detection with a similar detection limit to the normal PCR, and showed good stability of encapsulated PCR nanomaterial after storage for a week.

Since its discovery in 1986, polymerase chain reactions (PCR) have been one of the most important techniques in molecular biology to exponentially amplify target DNA [1], which is commonly used in bioanalytical, biomedical and biotechnological fields for the detection of genetic diseases, identification of genetic fingerprints, diagnosis of infectious diseases, cloning of genes, and paternity testing [2–8]. In the recent Covid-19 pandemic, PCR is still the gold standard for screening early infections [9,10].

A PCR reaction contains not only a DNA polymerase and dNTPs but also a set of primers. These reagents are stored separately and mixed with buffer and a template DNA for reaction. PCR reagents need to be stored at −20 °C and for a typical detection reaction, a lot of mixing steps are needed [11]. To improve the efficiency and speed of the amplification in a parallel manner, some researchers encapsulated PCR reagents in liposomes, emulsion droplets or polyelectrolyte microcapsules, which can be used as "nanoreactors" to perform biomolecular reactions for gene delivery application [12–17]. Some labs also freeze-dried reagents stored in polymer PCR chips for long-term stability of the reagents [18,19]. Some other methods such as real-time PCR [20], PCR-immune colloidal gold strip technology [21], loop-mediated isothermal amplification [22], digital PCR [23], and reverse transcription quantitative PCR [24] were also developed for improvement of the conventional PCR method.

A typical PCR reaction is comprised of deoxynucleoside triphosphates (dNTP, ~0.2 mmol/L), primers (~1 μmol/L) and a DNA polymerase (~12.5 IU). The template or target DNA to be amplified is typically at very low concentrations (nmol/L or lower level) [25]. Therefore, the main components are dNTP and primers. It has been recently shown that various transition metal ions and lanthanides can assemble various nucleotides to form coordination materials [26–29]. In addition, DNA can also participate in such reactions, and the formation of Fe/DNA nanoparticles is an interesting example [30,31]. Metal coordination can in turn stabilize DNA at high temperatures [32]. Since both dNTP and primers are in high concentrations in PCR, we wondered whether it is possible to use these intrinsic components of PCR reagents to form a coordination material to contain all the reagents, which may be suitable for storage, handling and integration of PCR reactions.

To investigate whether metal ions can encapsulate PCR reagents by forming coordination nanomaterials while still allowing PCR amplification, a few common transition metal ions were respectively incubated with PCR reagents (dNTP, primers and DNA polymerase) at room temperature for 1 h and centrifuged to remove the nonencapsulated reagents in the supernatants (Fig. 1A). Af-

* Corresponding authors.
E-mail addresses: zhengjinkai@caas.cn (J. Zheng), liujw@uwaterloo.ca (J. Liu).

https://doi.org/10.1016/j.cclet.2023.108808
1001-8417/

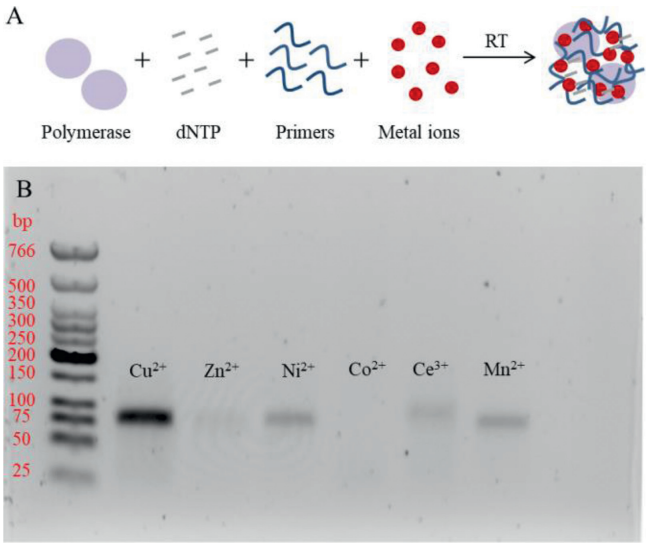

Fig. 1. (A) A scheme showing the assembly and encapsulation of PCR reagents using metal coordination. The non-incorporated molecules were removed. (B) A gel micrograph showing the performance of PCR reagents assembled using 4 mmol/L different metal ions. The template DNA concentration was 10 nmol/L.

ter that, EDTA was added to dissolve the nanoparticles for releasing the PCR reagents. An 80-mer template DNA and buffer were then added to the samples, and PCR reactions were carried out in a thermocycler as normal. Finally, agarose gel electrophoresis was performed for product analysis. As shown in Fig. 1B, a high yield of PCR products was achieved with Cu^{2+} but little with the other metals including Zn^{2+}, Ni^{2+}, Co^{2+}, Ce^{3+}, and Mn^{2+}, indicating Cu^{2+} may assemble the PCR reagents to form coordination materials. The position of the PCR product bands was at the expected position based on the ladder. So, Cu^{2+} was chosen as an optimal metal for the subsequent studies. For the other metal ions, it is known that Ni^{2+}, Co^{2+} and Ce^{3+} can strongly interact with DNA [33,34], whereas the interaction might be too weak for Mn^{2+} and Zn^{2+}. Cu^{2+} has the optimal affinity.

To quantitatively understand the effect of PCR reagents assembly by Cu^{2+}, we first optimized the concentration of Cu^{2+}. Different concentrations of Cu^{2+}were added for encapsulating PCR reagents and then PCR thermocycling was conducted. The yield of the PCR product peaked when 4 mmol/L Cu^{2+} was used, after which the yield decreased as Cu^{2+} was further increased (Figs. 2A and B). We reasoned that Cu^{2+}participated in the formation of the coordination reactions. Thus, the more Cu^{2+}, the more PCR reagents encapsulated. However, too much metal ions may also inhibit the PCR efficiency [35]. The inhibition effect of high concentrations of Cu^{2+} was verified by performing the normal PCR reaction in the presence of different concentrations of Cu^{2+}, where 1 mmol/L Cu^{2+} significantly inhibited the reaction (Fig. S1 in Supporting information). Note that while 4 mmol/L Cu^{2+} was added to form coordination nanomaterials with dNTP and PCR primers, not all the added Cu^{2+} ions were incorporated. The encapsulated efficiency of Cu^{2+} was calculated to be about 20% (Fig. S2 in Supporting information), and thus about 0.8 mmol/L Cu^{2+} was incorporated, which did not inhibit the reaction.

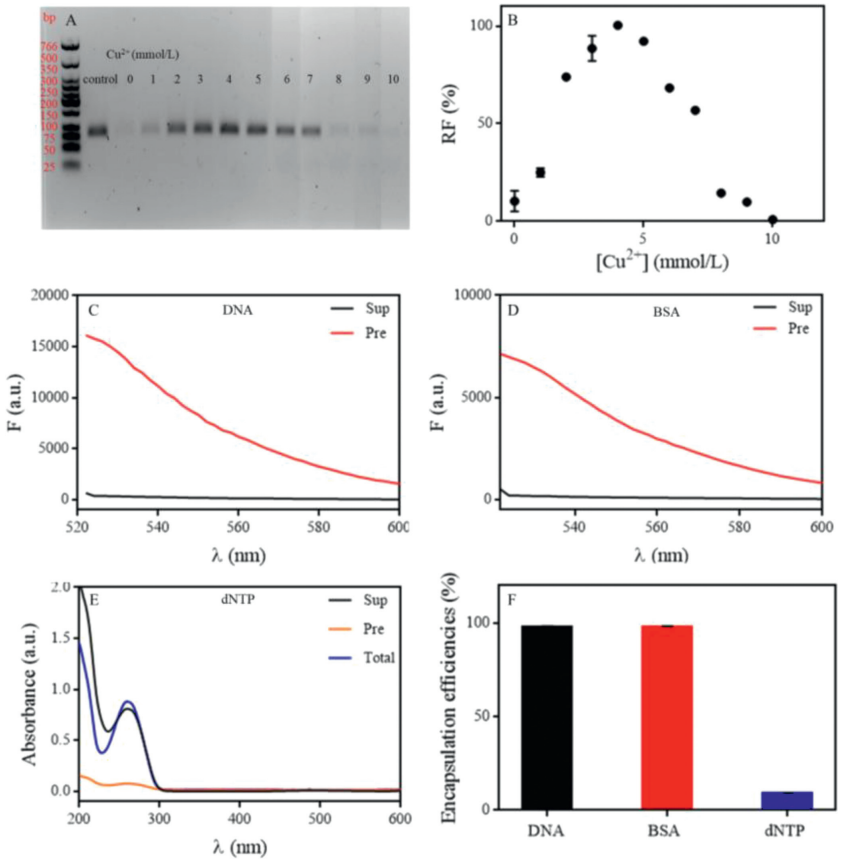

Fig. 2. (A) A gel micrograph showing the PCR products using the Cu^{2+}-assembled reagents with different Cu^{2+} concentrations. (B) Quantification of the results in (A) and 4 mmol/L Cu^{2+} is optimal. UV–vis and fluorescence spectra to calculate the encapsulation efficiency of (C) the primers, (D) FITC-BSA as a polymerase surrogate, and (E) dNTP. (F) The encapsulation efficiencies.

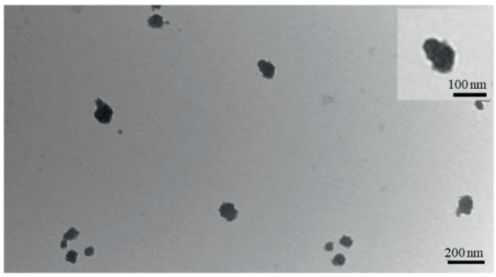

Fig. 3. A TEM micrograph of the Cu^{2+} and PCR reagents formed nanoparticles.

We also optimized the concentration of primer and dNTP for the normal PCR and PCR using Cu^{2+}-coordination nanoparticles (Fig. S3 in Supporting information). The results showed the yield of PCR products increased as the primer or dNTP concentration increased. Without Cu^{2+}, the optimal dNTP concentration was 0.2 mmol/L, and up to 4 μmol/L primer can be used. For the Cu^{2+}-mediated nanoparticles, more products were formed with higher dNTP concentrations, while the optimal primer concentration was 2 μmol/L. Overall, the optimal condition for the Cu^{2+} mediated PCR and normal PCR was quite similar.

We then used a FAM-labeled 24-mer DNA oligonucleotide to evaluate the encapsulate efficiency of DNA primers. The FAM-labeled DNA (1 μmol/L) and primer DNAs (1 μmol/L) were mixed and incubated with Cu^{2+}, dNTP and DNA polymerase to form the coordination nanomaterials. The samples were then centrifuged and the fluorescence of supernatant and dissolved precipitates were measured. The fluorescence of the dissolved precipitates was much higher than that of supernatant and the DNA encapsulate efficiency was calculated to be as high as 98%, indicating almost all the DNA primers were in the precipitant nanoparticles (Fig. 2C).

To evaluate polymerase encapsulation efficiency, we used FITC-labeled bovine serum albumin (BSA) to estimate the protein encapsulate efficiency for the formed coordination nanomaterial. Using the same method, about 98% BSA was in the precipitant, indicating a high encapsulate efficiency of protein (Fig. 2D). From this, we speculated the formed coordination nanomaterials can encapsulate nearly all the polymerase to conduct the PCR reaction. A high protein incorporation efficiency was also observed for other metal/nucleotide complexes [36]. It is reported that the phosphate and the base in DNA nucleotides can be involved in metal coordination [37], and Cu^{2+} has an optimal affinity to DNA [38], which can result in full coordination of DNA with Cu^{2+} ions.

Finally, the encapsulate efficiency of dNTP was measured by UV–vis absorption spectroscopy as dNTPs display a characteristic absorption peak at 260 nm. Since almost all the DNA primers were encapsulated in the precipitant, the absorption peak at 260 nm can be assigned to dNTP. Fig. 2E shows that only a small amount of dNTP was in the precipitant and the encapsulate efficiency was about 10%. The low encapsulate efficiency of dNTP may be attributed to the excess dNTP in solution, but the small amount dNTP was still enough for the PCR reaction. We summarized the encapsulation efficiency of each component in Fig. 2F. According to the data, before forming the nanomaterials, the ratio of enzyme, primer, and dNTP was 12.5 IU: 2 μmol/L: 200 μmol/L, whereas after forming the integrated PCR nanomaterials, the ratio was 12.5 IU: 2 μmol/L: 20 μmol/L.

The morphology and size of the coordination nanoparticles were further characterized by TEM (Fig. 3). The obtained nanopar-

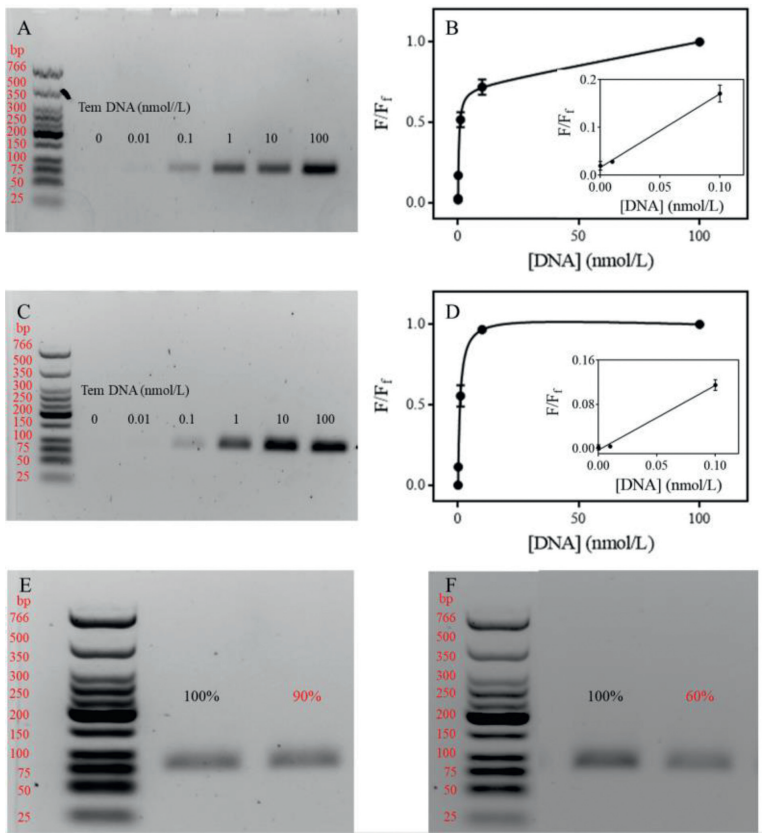

Fig. 4. PCR products of (A, B) the encapsulated nanoparticles compared with (C, D) the normal PCR in the presence of different concentrations of the target template DNA. *F* represents the fluorescence of each point, and F_f means the fluorescence when DNA concentration was 100 nmol/L. The PCR efficiency of (E) the proposed system and (F) the conventional PCR method after one-week storage.

ticles had a rough surface and were about 100 nm in size. It seemed that many small nanoparticles clustered together to form the assembled nanoparticles. DLS showed the size of the nanoparticle to be about a few hundred nanometers, which was consistent with the TEM experiment. The measured size became smaller after drying and re-dispersion (Fig. S4A in Supporting information). The size of the coordination nanoparticles is also influenced by Cu^{2+}, *i.e.*, the more copper, the larger the particle size (Fig. S5 in Supporting information).

After treated with 1 mmol/L EDTA, the nanoparticles were dissolved. We used 1 mmol/L EDTA to chelate Cu^{2+}, but some Mg^{2+} still remained for the PCR reaction, since the formation constant of EDTA/Cu^{2+} is about 10 orders of magnitude larger than that of EDTA/Mg^{2+}. A low concentration of EDTA actually increased the PCR efficiency, but with 2 mmol/L EDTA, the PCR efficiency was significantly inhibited (Fig. S6A in Supporting information). This result can be explained by EDTA chelation of Mg^{2+}in the PCR reaction buffer. Mg^{2+} was required in the PCR reaction, but a high concentration of Mg^{2+} may inhibit the reaction by mechanisms like binding to dNTP or increasing the melting temperature of DNA too much. In our system, the PCR efficiency dropped drastically when more than 10 mmol/L Mg^{2+} was added (Fig. S6B in Supporting information).

We then investigated the PCR performance of the encapsulated nanoparticles. The PCR regents were encapsulated into the Cu^{2+}nanoparticles. After centrifugation and drying, the formed nanoparticles were treated with EDTA and dispersed in buffer and different concentrations of the target template DNA were added to perform PCR. As shown in Figs. 4A-D, the PCR products increased as the concentration of DNA template changed from 0 to 100 nmol/L, and the detection limit was 17 pmol/L, which was similar to the normal PCR (10 pmol/L), confirming good performance of the encapsulated nanoparticles (Table S1 in Supporting information).

To investigate the stability of the formed nanoparticles, we dried the nanoparticles, rehydrated them with buffer and then run the PCR. After drying, the nanoparticles deposited at the bottom of the tube and had obvious green color indicative of Cu^{2+} coordination, while the normal PCR regents showed no color (Fig. S4B in Supporting information). After running gel, the yield of PCR products was slightly lower compared with the normal PCR.

We also measured the PCR efficiency of the proposed system after long-time storage compared with the conventional PCR method. The PCR efficiency for the proposed system after a week was measured to be 90% of the original system, while for the normal PCR, the efficiency decreased to be 60% (Figs. 4E and F), suggesting better storage stability of the proposed system.

In conclusion, we screened a few transition metal ions to form coordination nanomaterials with dNTP and DNA primers and encapsulate DNA polymerase, forming an integrated PCR reaction system. For the detection, users only need to dissolve the coordination nanomaterials with buffer and EDTA and add a template DNA for PCR amplification. Cu^{2+} was found to be the most effective metal ion for this purpose, and the encapsulation efficiency reached close to 100% for the primers and DNA polymerase, although only around 10% of dNTP was incorporated. This is the first work to use both dNTP and DNA oligonucleotides to form coordination polymers and it is an interesting system to simplify PCR reactions.

Declaration of competing interest

The authors declare that they have no known competing financial interests or personal relationships that could have appeared to influence the work reported in this paper.

Acknowledgments

Funding for this work was from the Natural Sciences and Engineering Research Council of Canada (NSERC), the National Natural Science Foundation of China (Nos. 31901776 and 32072181), and Agricultural Science and Technology Innovation Program (No. CAAS-ASTIP-2021-IFST-SN2021-05). C. Lu received a China Scholarship Council (CSC) Scholarship to visit the University of Waterloo.

Supplementary materials

Supplementary material associated with this article can be found, in the online version, at doi:10.1016/j.cclet.2023.108808.

References

[1] Y. Liu, G. Yang, T. Li, et al., Chin. Chem. Lett. 32 (2021) 1957–1962.
[2] M. Kidd, A. Richter, A. Best, et al., J. Infect. Dis. 223 (2021) 1666–1670.
[3] K.R. Sreejith, C.H. Ooi, J. Jin, et al., Lab Chip 18 (2018) 3717–3732.
[4] R. Yamashige, M. Kimoto, R. Okumura, I. Hirao, J. Am. Chem. Soc. 140 (2018) 14038–14041.
[5] S.Q. Bonny, M.M. Hossain, S.M.K. Uddin, et al., Crit. Rev. Food Sci. Nutr. 62 (2022) 1317–1335.
[6] H. Li, R. Bai, Z. Zhao, et al., Biosci. Rep. 38 (2018) BSR20181170.
[7] M. Lescat, L. Poirel, P. Nordmann, Diagn. Microbiol. Infect. Dis. 92 (2018) 267–269.
[8] X.Y. Jin, Y.Y. Wei, W. Cui, et al., Electrophoresis 40 (2019) 1691–1698.
[9] Á. Beltrán-Corbellini, J. Chico-García, J. Martínez-Poles, et al., Eur. J. Neurol. 27 (2020) 1738–1741.
[10] L.Le Cleach, L. Dousset, H. Assier, et al., Br. J. Dermatol. 183 (2020) 866–874.
[11] P.J.J. Huang, J. Liu, ChemistryOpen 9 (2020) 1046–1059.
[12] G. Baier, A. Musyanovych, M. Dass, et al., Biomacromolecules 11 (2010) 960–968.
[13] G. Baier, A. Musyanovych, V. Mailander, K. Landfester, Int. J. Artif. Organs 35 (2012) 77–83.
[14] F. Cavalieri, A. Postma, L. Lee, F. Caruso, ACS Nano 3 (2009) 234–240.
[15] A. Price, A. Zelikin, K. Wark, F. Caruso, Cell. Polym. 29 (2010) 197–198.
[16] W.C. Mak, K.Y. Cheung, D. Trau, Adv. Funct. Mater. 18 (2008) 2930–2937.
[17] A.N. Zelikin, A.L. Becker, A.P. Johnston, et al., ACS Nano 1 (2007) 63–69.
[18] D. Chen, M. Mauk, X. Qiu, et al., Biomed. Microdevices 12 (2010) 705–719.
[19] J. Kim, D. Byun, M.G. Mauk, H.H. Bau, Lab Chip 9 (2009) 606–612.
[20] J. Garg, V. Singh, P. Pandey, et al., J. Med. Virol. 93 (2021) 1526–1531.
[21] R. Yin, Y. Sun, K. Wang, et al., Food Chem. 318 (2020) 126541.
[22] X. Jiang, M. Yang, J. Liu, ACS Appl. Mater. Interfaces 14 (2022) 27666–27674.
[23] H. Chen, X. Ma, X. Zhang, et al., Chin. Chem. Lett. 34 (2023) 107701.
[24] N.R. Blumenfeld, M.A.E. Bolene, M. Jaspan, et al., Nat. Nanotechnol. 17 (2022) 984–992.
[25] L. Wang, Z. Huang, R. Wang, et al., ACS Appl. Mater. Interfaces 10 (2018) 4409–4418.
[26] J. Zhou, H. Han, J. Liu, Nano Res. 15 (2022) 71–84.
[27] Z. Huang, B. Liu, J. Liu, Chem. Commun. 56 (2020) 4208–4211.
[28] R. Nishiyabu, N. Hashimoto, T. Cho, et al., J. Am. Chem. Soc. 131 (2009) 2151–2158.
[29] Q. Ma, F. Li, J. Tang, et al., Chem. Eur. J. 24 (2018) 18890–18896.
[30] M. Li, C. Wang, Z. Di, et al., Angew. Chem. Int. Ed. 58 (2019) 1350–1354.
[31] Z. Zou, L. He, X. Deng, et al., Angew. Chem. Int. Ed. 133 (2021) 23152–23158.
[32] C. Lu, Y. Xu, P.J.J. Huang, et al., Nanoscale 14 (2022) 14613–14622.
[33] B. Liu, J. Liu, ACS Appl. Mater. Interfaces 7 (2015) 24833–24838.
[34] L. Chen, B. Liu, Z. Xu, J. Liu, Langmuir 34 (2018) 9314–9321.
[35] A. Kuffel, A. Gray, N.N. Daeid, Int. J. Legal. Med. 135 (2021) 63–72.
[36] H. Liang, S. Jiang, Q. Yuan, et al., Nanoscale 8 (2016) 6071–6078.
[37] H. Liang, Z. Zhang, Q. Yuan, J. Liu, Chem. Commun. 51 (2015) 15196–15199.
[38] M. Košćak, I. Krošl, B. Žinić, I. Piantanida, Chemosensors 10 (2022) 34.